Springer

Journal of Mechanical Science and Technology 23 (2009) 1563~1570

Journal of Mechanical Science and Technology

www.springerlink.com/content/1738-494x
DOI 10.1007/s12206-009-0418-0

Molecular dynamic simulation of the melting and solidification processes of argon †

Jae Dong Chung*

Department of Mechanical Engineering, Sejong University, Seoul, 143-747, Korea

(Manuscript Received June 24, 2008; Revised February 25, 2009; Accepted April 9, 2009)

Abstract

Molecular Dynamic (MD) simulations have been conducted to look at the melting and solidification of the Lennard-Jones argon (100) interface with small amounts (up to 6.0K) of undercooling and superheating. By combining the fully equilibrated bulk phases of liquid and solid in one simulation box and counting the number of solid–like particles, the interface velocities, i.e. the growth rate or melting rate, were obtained as a function of temperature. The melting temperature, where no growth or melting of crystal particle is expected, is T_m^* =0.668 which is close to that of the Gibbs free energy calculation. A linear dependence of growth or melting rate on temperature was found except for high superheating, ΔT > 6K. The high superheating is believed as the main source of slope discontinuity in the rate, not the misuse of initial regime as discussed in the earlier works.

Keywords: Phase transition; Freezing rate; Molecular dynamic simulations; Melting temperature

1. Introduction

The study of the growth rates of crystals from the melt or from supersaturated solutions is of importance for the prediction of their macroscopic growth morphologies. Although much is known about the thermodynamics of the solid–liquid phase transition, the kinetics of this transition are still poorly understood. Since probing the interface between two dense phases is largely inaccessible with experimental techniques [1], the atomistic details from computer simulations have provided an excellent alternative for understanding the microscopic processes involved in crystallization or melting.

One of the open questions on phase transitions concerns the rates of growth and melting. There has been much debate on whether there exists a slope discontinuity in the rates when crossing the melting point. Uhlmann et al. [2] ascertained that an abrupt change in the kinetic coefficient would imply a violation of microscopic reversibility. However, the asymmetry of freezing and melting kinetics was shown experimentally for crystalline silicon by Tsao et al. [3]. Their results were supported by several researchers [4-6]. Even the same research group, however, reported contradictory results [7, 8]. They explained this in terms of lattice imperfections.

In this study, molecular dynamic (MD) simulations were used to look at the melting and solidification of argon at small amounts (6.0K) of undercooling and superheating. Special care was taken at the melting temperature and for the rates of growth and melting at the Lennard-Jones (100) interface.

2. System and simulation method

The argon FCC (100) interface was chosen as the simulation system, which is commonly described by a Lennard-Jones potential. Choosing a simple system allows for the elucidation of results that may be difficult to resolve in more complex materials, where

† This paper was recommended for publication in revised form by Associate Editor Dongsik Kim

*Corresponding author. Tel.: +82 2 3408 3776, Fax.: +82 2 3408 4333
E-mail address: jdchung@sejong.ac.kr

multi-atom unit cells can generate additional effects. The Lennard-Jones 6-12 potential describing the two-body interaction between atoms i and j separated by distance r_{ij}, is

$$\phi\left(r_{ij}\right)=4\varepsilon\left[\left(\frac{\sigma}{r_{ij}}\right)^{12}-\left(\frac{\sigma}{r_{ij}}\right)^{6}\right] \tag{1}$$

where σ and ε define characteristic length and energy scales, respectively. The potential ϕ is 0 at $r_{ij}=\sigma$ and its minimum is $-\varepsilon$ at $r_{ij}=2^{1/6}\sigma$. Argon has values σ = 3.405 Å and ε/k_B = 119.8 K. The parameters ε and σ are used as units of energy and length, respectively. Simulation results have been reported in reduced units such as $N^*=N\sigma^3/V$, $T^*=k_BT/\varepsilon$, $E^*=E/\varepsilon N$, $t^*=t/\left(m\sigma^2/\varepsilon\right)^{1/2}$, $P^*=P\sigma^3/\varepsilon$.

Baidakov et al. [9] pointed out that the cut-off radius of the interaction potential in two-phase systems is extremely important and should be chosen to be larger (6.78σ in their study) than that for the one-phase systems to provide an adequate representation of properties. But in contrast to their liquid-gas system, the density change between liquid-solid is not as large as that between vapor-liquid, so the cut-off radius is not expected to be as sensitive as liquid-gas system. From the experience in one-phase systems and 2.5σ used in Tepper and Briels [8], the atomic interactions were truncated at a cutoff radius of 3.5σ, which is nearly one-half of the length of the simulation box.

Periodic boundary conditions were imposed in all directions. The classical trajectories of the atoms were determined by using the Verlet leap-frog integration algorithm [10] with a time step of 2 fs. One should carefully choose the time step so that all the time-scales of interest in the system can be resolved. In simulations of LJ argon where the highest frequency is 2 THz, a time step of 2 fs is sufficiently small compared to typical values of 5~10 fs [11]. The effect of the time step was investigated compared with 1 fs time step and with the same heating/cooling rate, no appreciable difference was found.

The size effect on melting and crystallization was explored over the range of 500~1372 atoms. This showed negligible differences for typical heating and cooling rates, so a simulation box composed of $5\times5\times5$ FCC unit cells (500 atoms) was adopted.

All the MD simulations presented here were carried out, except where noted, in the isobaric-isothermal (NPT) ensemble. The pressure was kept constant at atmospheric pressure, P^* = 0.002418 by a Nosé-Hoover method [12] and Langevin dynamics [13]. The thermostat relaxation time and barostat relaxation time were chosen as 200 fs and 100 fs, respectively. The melting was achieved by a step-wise increase of the system temperature ΔT = 0.5K, initially FCC crystal well below its estimated melting temperature. Between increments, the temperature was held constant and the simulation was run for 30,000 steps; thus the heating rate is 8.33×10^9 K/s. The heating rate was varied over the range 8.33×10^9 K/s to 8.33×10^8 K/s (=0.1K/120ps) to examine its effect on the melting temperature. The same was done when cooling the melt. All temperature dependent intensive properties have been averaged after one-third of total simulation time steps at each temperature which is enough for equilibration.

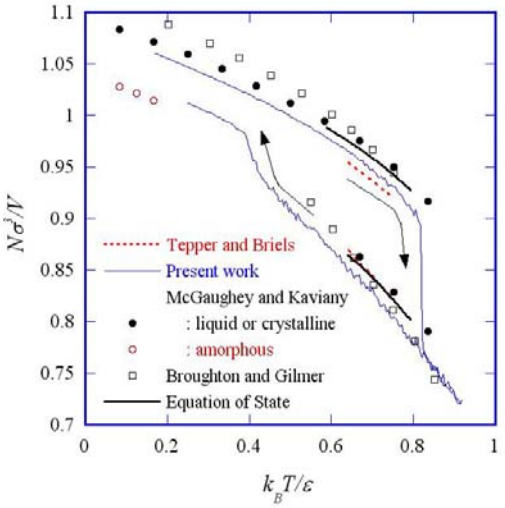

Fig. 1. Number density variations in the heating and cooling process at 8.33×10^9 K/s.

3. Melting temperature

The number densities of the solid and liquid phases are plotted as a function of temperature in Fig. 1. Upon incremental heating, the number densities of the system increases steadily until there appears a catastrophic volume increase at T_m^+ =0.818. The excellent agreement between the value obtained here and other reported values [8, 11, 14-16], validates the method and simulation code employed. Deviations from other research are expected because of the simulation box

size, cutoff radius and potential shift. Another validation was done by comparing the zero temperature unit cell parameter. When relaxed to zero temperature, the MD FCC crystal unit cell parameter is 5.2686 Å, which corresponds to a cutoff radius of 3.5 σ. McGaughey and Kaviany [11] have found values of 5.2414 Å for a cutoff radius of 3.1 σ. The experimental value is 5.3033 Å [17].

Previously, the discontinuity in the potential energy or volume vs. temperature curve was inappropriately assumed as an indicator of melting. However, we should distinguish the thermodynamic melting T_m^* which occurs heterogeneously, and melting due to mechanical instability T_m^+ [18], which is a homogeneous process. Since, due to superheating, T_m^+ can be considerably higher than T_m^*, any failure to distinguish between these two quantities will result in confusion in interpreting the melting characteristics of the model system. In contrast to an experiment in which superheating is extremely difficult even in the most favorable cases, numerical simulations of a perfect-crystal cell allow substantial metastable overheating without suffering from heterogeneous nucleation sites. Several measurements demonstrate that when the surface conditions are modified, the melting point can be depressed [19] or the solid can be substantially superheated [20]. This implies that melting is basically a heterogeneous process and the temperature obtained from the MD results of the abrupt volume change is a mechanical melting temperature, not a thermodynamic one. Note that even after long runs (up to 1×10^6 time steps) above T_m^* such as T^*=0.78, no signal for melting can be detected, indicating the existence of substantial metastable superheating.

Since the equilibrium state is the state of minimum Gibbs free energy, free energy calculations should be performed to determine the thermodynamic melting point T_m^*, which is defined as the temperature at which the free energies of the crystalline and liquid phases are equal. Computation of both free energy differences and absolute free energies has prompted a great deal of attention and techniques such as free energy perturbation [21] and thermodynamic integration [22] have been well-established. However, the computational implementation poses formidable barriers to its practical use, and the proper convergence of the free energy calculations and quantitative interpretation of the results require extremely long simulations. Thus, the densities of each phase were used to simply evaluate the free energies of the solid and liquid from the equations of state. The expressions were adopted for the liquid from Johnson et al. [15] and for the solid from Hoef [16]; these are known to be most accurate expressions for each phase.

The number density of the bulk FCC crystal as a function of temperature in the range from 75K to 87K (i.e., $0.6260 < T^* < 0.7262$) at $P^* = 0.002418$ can be fitted from Fig. 1 with a second-order polynomial:

$$N_s^* = -0.33302 + 0.05106\times T - 0.00064085\times T^2 + 2.5488\times10^{-6}T^3 \quad (2)$$

with a coefficient of determination $R^2 = 0.99693$. For the bulk liquid, the number density for the same temperature range is given by

$$N_l^* = -6.5427 + 0.2847\times T - 0.0036066\times T^2 + 1.5015\times10^{-5}T^3 \quad (3)$$

with a coefficient of determination $R^2 = 0.99145$. Applying these densities to the equations of state for each phase gives the melting temperature 82.4K (T_m^*=0.6878). The thermodynamic melting point is 82.28K from a simulation [23] and 83.8K from experiment [24]. The thermodynamic melting point determined here by the Gibbs free energy is very close, but not exactly the same as the experimental value because the potential function does not describe Ar perfectly and the cutoff is used.

In the heating process, the solid phase is maintained above the thermodynamic melting temperature, until the mechanical melting temperature is reached where collapse of the crystal lattice occurs due to the elastic instability associated with an unstable phonon mode. Also, the liquid phase is maintained below the thermodynamic melting temperature in the cooling process, giving clear hysteresis as shown in Fig. 1. Luo et al. [25] suggested the "hysteresis method" where T_m^* can be deduced given the temperature for the maximum degree of superheating (T_m^+) and undercooling (T_m^-) as

$$T_m^* = T_m^+ - \sqrt{T_m^+ T_m^-} + T_m^- \quad (4)$$

They ascertained that the deviation of their hysteresis method was about 2% or less. However, we cannot find any physical explanation for this method and the melting temperature evaluated from the data in

Fig. 1, T_m^*=0.652 is far from the experimental observation.

The effect of heating rate and cooling rate was scrutinized for four different rates, 0.5K/60ps, 0.25K/60ps, 0.25K/120ps, and 0.1K/120ps and Fig. 2 shows the energy variations. No significant differences were found except for the cooling process at 8.33×10^9 K/s. We find that at high cooling rate, this solid phase is not crystalline but amorphous as shown in Fig. 1 where solidification occurs but number density differs from crystalline. Nosé and Yonezawa [26] showed that there is a critical cooling rate which separates crystal-forming and glass-forming. McGaughey and Kaviany [11] also found an amorphous phase by quenching at a high cooling rate, 8.5×10^{11} K/s, shown in Fig. 1 as open circle symbols. However, they argued that above 20K the thermal equilibrium fluctuations in the system are large enough to return the atoms to the FCC crystal structure. In the present work, the amorphous phase is maintained up to 45K.

The heat of melting may also be obtained from the difference in the configurational energy between the crystalline and liquid phases at the melting point. In Fig. 2, the calculated value of the latent heat is 1.12 kJ/mol, which is compatible with the experimental value of 1.18 kJ/mol.

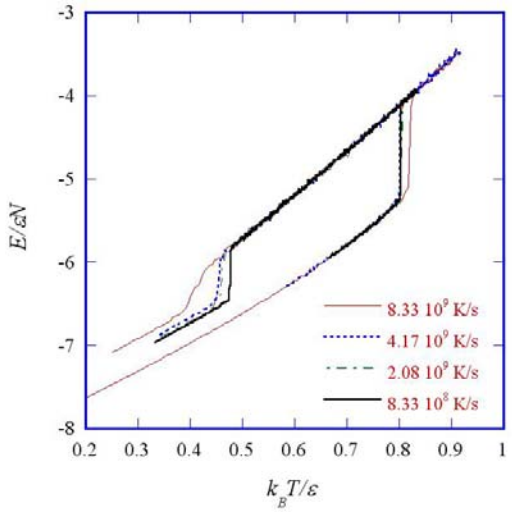

Fig. 2. Energy variations in the heating and cooling process at various heating/cooling rates.

4. Growth and melting rate

Growth and melting rate are also examined using combined simulation boxes of the solid and liquid phases at the expected melting temperature. If the given temperature is higher than the melting temperature, the interface between solid and liquid phases will move towards the solid phase; if the given temperature is lower than the melting temperature, the direction of the interface movement will be opposite. By counting the number of solid–like particles, we can estimate the interface velocity, i.e., the growth rate or melting rate, as a function of temperature.

In combining the fully equilibrated bulk phases of the liquid and solid in one simulation box, it is reported that the proper preparation of the two-phase system plays a crucial role in determining the resulting growth and melting rates [8]. In the present work, an NPT simulation was initially carried out for solid phase at the expected (i.e., experimental) melting temperature T^*=0.6995 and a time-averaged volume was obtained. Then the bulk NVT simulation at this volume was run for 100,000 time steps of equilibration and was written once every 1,000 time steps for 15,000 further time steps. For the liquid phase, the same procedure was conducted by fixing the cross-section area in the x-y plane to be equal to the time-averaged value of the solid phase. Thus, only the z-directional volume change can be permitted in the NPT simulation. After equilibration in NVT, the results were written once every 1,000 time steps. To make two-phase boxes, one liquid configuration and one solid configuration were taken, and both copied twice in the $z-$direction in the order liquid-solid-solid-liquid. The resulting system contained two solid-liquid interfaces and consisted initially of 1,000 solid particles ($5\times5\times10$ unit cells) and 1000 liquid phase particles.

To release excessive potential energy due to particle overlap, 10,000 time steps with the NVT simulation were conducted on condition that the solid phase atoms remained frozen at their positions. After this, the combined two-phase systems were quenched to the desired temperature and NPT runs were carried out to study growth and melting rates. The volume relaxation in each direction took place independently. Due to volume fluctuations in the isothermal-isobaric ensemble, the simulation was repeated for 15 runs from different starting configurations and subsequently averaged to obtain good statistical accuracy. Since the fluctuation of the solid-like particle number N_s in one single run was much less than that of Tepper and Briels [8] as shown in Fig. 5, only 15 runs of different starting configurations were regarded as

necessary. Note that Teppers and Briels used 50 runs. They pointed out that their approach of equilibration included the solid phase movement together with liquid phase movement and this had the side effect of removing imperfections that were present in the bulk crystal phase, which resulted in an asymmetry between growth and melting. In their other work, equilibration with a fixed solid phase was implemented but a much longer equilibration time was used. They emphasized that when equilibration was not carried out to its full extent, erroneous conclusions could be drawn about the temperature dependence of growth and melting rates.

The solid-like particle recognition criterion is based on the total instantaneous volume of the system. Since the volumes per particle for each phase are known from the bulk simulations, the proportion of particles between the solid and liquid phases can be calculated at every instance. The number of solid particles is estimated by

$$N_s(t) = \frac{N_{total}/N_l^* - V_{total}^*(t)}{1/N_l^* - 1/N_s^*} \tag{5}$$

where N_{total}, V_{total}^*, N_l^*, and N_s^* are the total number of particles, total volume normalized by σ^3, and particle number densities of liquid and solid, respectively.

Fig. 3 shows the growth and melting curves showing the number of solid-like particles vs. time along with curve-fitted lines for each temperature T^* = 0.6260, 0.6411, 0.6494, 0.6578, 0.6661, 0.6745, 0.6828, 0.6912, 0.6995, 0.7179. A change of slope is discernible for the temperature apart from the melting temperature as marked by the circle in Fig. 3, but is not obvious for temperatures close to equilibrium. Because of this change of slope, Tepper and Briels [8] suggested the presence of two regimes. They ascertained that the initial regime was associated with interface relaxation and the second regime was associated with the macroscopic limit of growth and melting and true growth and melting rates should be obtained from the second regime. With the data of the second regime, they showed that there was no discontinuity in the melting and growth rates. However, they did not show any clear reason why the slope change of N_s occurs. Also, the distinction between the two regimes may be ambiguous since, as they pointed out, the second regime was not found close to equilibrium.

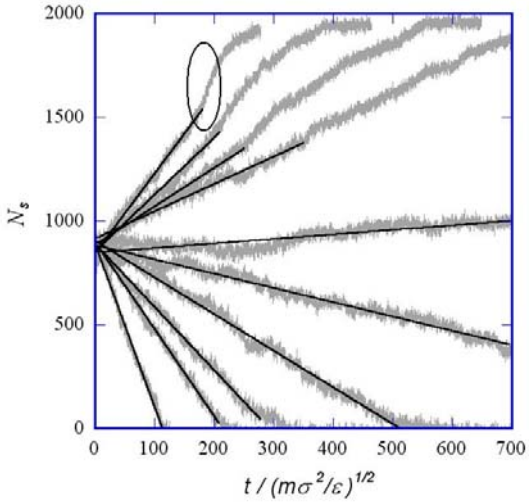

Fig. 3. Growth and melting curves showing the number of solid-like particles vs. time for temperatures T^* = 0.6260, 0.6411, 0.6494, 0.6578, 0.6661, 0.6745, 0.6828, 0.6912, 0.6995, 0.7179.

In addition, the second regime existed only for a very short time when far from equilibrium.

The temperature dependence of the rates as determined from the slopes of the average melting curves is presented in Fig. 4. The present work shows a linear dependency on temperature. It is hard to say if the two fitted lines above and below the melting temperature in Fig. 4 have different slopes considering the uncertainties involved in the MD simulations. Note that the simulation box with 2,000 atoms is much smaller than those of Tepper and Briels [8] which had 4048 and 8096 atoms. They ascertained that the second regime could only be measured accurately for sufficiently large systems and a non-linear melting rate might appear in a small simulation box. However, if the data furthest from the melting temperature ΔT =6.0K is excluded, their results for the initial regime also show a clear linear dependency with a coefficient of determination R^2 = 0.99954. This is clearly in conflict with their conclusion. Thus, a reassessment will be needed on the slope discontinuity to determine whether it stems from the initial simulation regime or high superheating.

In Fig. 4, the initial regime has different phase change rate from that of long-time regime. Which rate is true phase change rate is another problem, but we can see no slope discontinuity in the growth and melting rates in the long-time regime but also in the initial regime for the all results of the present and Tepper and Briels [8]. The reason for the appearance of two

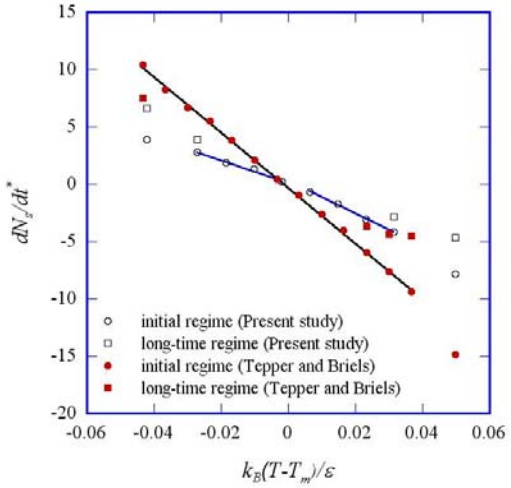

Fig. 4. Melting rates as a function of temperature, determined from the slopes of the average melting curves.

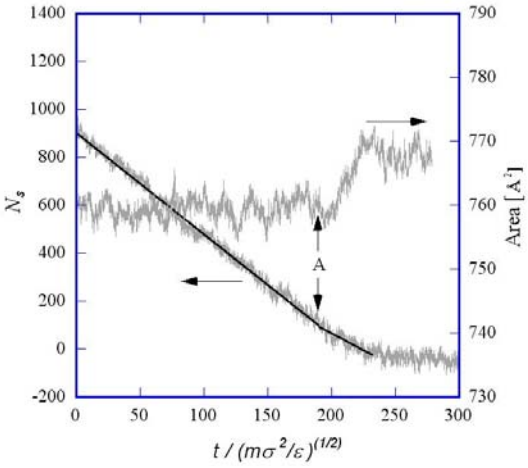

Fig. 5. Melting curves showing the number of solid-like particles and cross sectional area vs. time at T^* =0.6995.

regimes can be understood by examining the cross sectional area change together with the change in the number of solid-like particles as shown in Fig. 5. Although independent volume relaxations in the $x-$, $y-$, $z-$directions were allowed, the area of the $x-y$ plane remains constant for a time because the $z-$direction is much more flexible than the $x-$ or $y-$directions, which are restricted by the solid phase. After some time, the flexibility of the $x-$, $y-$, $z-$directions becomes comparable, and each directional contribution to the volume increase becomes similar. The distinction between the two regimes suggested by Tepper and Briels [8] coincides with the abrupt area change at time indicated by arrow A in Fig. 5 where the area of the $x-y$ plane starts to increase. Care should be taken when evaluating the growth rate in the second regime since a variable cross sectional area also affects the growth rate, $R = 1/(2\rho_s A)\cdot dN_s/dt$, as well as the evolution of the number of solid particles. This was not considered by Tepper and Briels [8].

The melting temperature, where no growth or melting of the crystal particles in Fig. 4 is expected, is T_m^* =0.668. This value is close to that from the Gibbs free energy calculation. At this temperature, a snapshot of the atomic configuration and sectional number density variation is shown in Fig. 6. The sectional number density distribution is obtained by averaging 80 time frames in each slice along the $z-$direction, with its width is chosen to be 1 Å. A broadening of the time-averaged interface profile is observed. Since

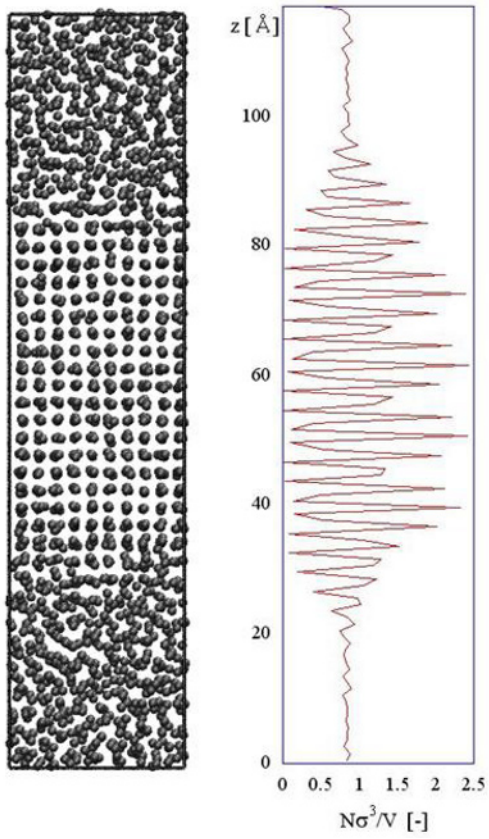

Fig. 6. Snapshot of the atomic configuration and sectional number density variation at the melting temperature T^* =0.668.

the Lennard-Jones FCC (100) crystal-melt interface is very diffuse [27], the interface extends over several interlayer spacings.

5. Conclusions

Molecular dynamic (MD) simulations have been carried out to look at the melting temperature and rates of growth and melting of the Lennard-Jones Ar (100) interface for small amounts (6.0K) of undercooling and superheating. Clear hysteresis behavior was found. The heating rate was varied over the range from 8.33×10^{9} K/s to 8.33×10^{8} K/s, and no significant differences were found for the mechanical melting point, but for the highest cooling rate (8.33×10^{9} K/s), an amorphous phase was observed. By combining the fully equilibrated bulk phases of liquid and solid in one simulation box and counting the number of solid–like particles, the interface velocity, i.e. growth rate or melting rate, was obtained as a function of temperature. A linear dependency on temperature was found except for high superheating, $\Delta T > 6$K. The high superheating is believed to be the main source of the slope discontinuity in the rate of growth or melting, not the misuse of initial regime as discussed in the earlier works. Initially the area of the $x-y$ plane remains constant due to the higher flexibility in the $z-$ direction; the distinction between the two regimes found in earlier work coincides with the point where the area of the $x-y$ plane starts to increase.

Acknowledgment

This work was supported by the Korea Research Foundation Grant funded by the Korea Government (MOEHRD) (KRF-2007-013-D00018)

Nomenclature

A : Area
E : Total energy
k_B : Boltzmann constant, 1.3806×10^{-23} J/K
m : Lennard-Jones mass scale
N : Number of atoms
P : Pressure
r : Particle position, interparticle separation
R : Growth rate
t : Time
T : Temperature
v : Volume per particle
V : Volume
x, y, z : Coordinate

Greek Symbols

ε : Lennard-Jones energy scale
ϕ : Potential energy
ρ : Number density
σ : Lennard-Jones length scale

Subscripts

i, j : Particle label
l : Liquid
m : Melting
s : Solid

Superscripts

* : Reduced unit
\+ : Superheat
— : Undercooling

References

[1] B. B. Laird and A. D. J. Haymet, The crystal/liquid interface: Structure and properties from computer simulation, *Chem. Rev.*, 92 (1992) 1819-1837.
[2] D. R. Uhlmann, J. F. Hays and D. Turnbull, The effect of high pressure on B2O3: Crystallization, desification, and the crystallization anomaly, *Phys. Chem. Glasses,* 8 (1967) 1-10.
[3] J. Y. Tsao, M. J. Aziz, M. O. Thompson and P. S. Peercy, Asymmetric melting and freezing kinetics in silicon, *Phys. Rev. Lett.,* 56 (1986) 2712-2715.
[4] M. D. Kluge and J. R. Ray, Velocity versus temperature relation for solidification and melting of silicon: A molecular-dynamics study, *Phys. Rev. B.,* 39 (1989) 1738-1746.
[5] M. Iwamatsu and K. Horii, Interface kinetics of freezing and melting of Si and Na, *Phys. Lett. A.,* 214 (1996) 71-75.
[6] C. J. Tymczak and J. R. Ray, Asymmetric crystallization and melting kinetics in sodium: A molecular-dynamics study, *Phys. Rev. Lett.,* 64 (1990) 1278-1281.
[7] H. L. Tepper and W. J. Briels, Simulation of crystallization and melting of the FCC (100) interface: the crucial role of lattice imperfections, *J. Crystal Growth*, 230 (2001) 270-276.
[8] H. L. Tepper and W. J. Briels, Crystallization and melting in the Lennard-Jones system: Equilibration, relaxation, and long-time dynamics of the moving interface, *J. Chem. Phys.,* 115 (2001) 9434-9443.
[9] V. G.. Baidakov, G. G. Chernykh and S. P. Protsenko, Effect of the cut-off radius of the intermolecular potential on phase equilibrium and surface tension in

Lennard-Jones systems, *Chem. Phys. Lett.,* 321 (2000) 315-320.
[10] M. P. Allen and D. J. Tildesley, *Computer simulation of liquid*, Oxford, 1987.
[11] A. J. H. McGaughey and M. Kaviany, Thermal conductivity decomposition and analysis using molecular dynamics simulations. Part I. Lennard-Jones argon, *Int. J. Heat Mass Transfer,* 47 (2004) 1783-1798.
[12] G. J. Martyna, D. J. Tobias and M. L. Klein, Constant pressure molecular dynamics algorithms, *J. Chem. Phys.,* 101 (1994) 4177-4189.
[13] S. E. Feller, Y. Zhang, R. W. Pastor and B. R. Brooks, Constant pressure molecular dynamics simulation: The Langevin piston method, *J. Chem. Phys.,* 103 (1995) 4613-4621.
[14] J. Q. Broughton and G. H. Gilmer, Molecular dynamics investigation of the crystal-fluid interface. I. Bulk properties, *J. Chem. Phys.,* 79 (1983) 5095-5104.
[15] J. K. Johnson, J. A. Zollweg and K. E. Gubbins, The Lennard-Jones equation of state revisited, *Mol. Phys.,* 78 (1993) 591-618.
[16] M. A. van der Hoef, Free energy of the Lennard-Jones solid, *J. Chem. Phys.,* 113 (2000) 8142-8148.
[17] O. G. Peterson, D. N. Batchelder and R. O. Simmons, Measurements of X-ray lattice constant, thermal expansivity, and isothermal compressibility of argon crystals, *Phys. Rev.,* 150 (1966) 703-711.
[18] M. Born and K. Huang, *Dynamical Theory of Crystal Lattices*, Oxford, 1962.
[19] Ph Buffat and J. P. Borel, Size effect on the melting temperature of gold particles, *Phys. Rev. A.,* 13 (1976) 2287-2298.
[20] J. Daeges, H. Gleiter and J. H. Perepezko, Superheating of metal crystals, *Phys. Lett. A.,* 119 (1986) 79-82.
[21] J. G. Kirkwood, Statistical mechanics of fluid mixtures, *J. Chem. Phys.,* 3 (1935) 300-313.
[22] R. W. Zwanzig, High-temperature equation of state by a perturbation method. I. Nonpolar gases, *J. Chem. Phys.,* 22 (1954) 1420-1426.
[23] R. Agrawal and D. A. Kofke, Thermodynamic and structural properties of model system at solid-fluid coexistence, *Mol. Phys.,* 85 (1995) 43-59.
[24] http://webbook.nist.gov
[25] S. N. Luo, A. Strachan and D. C. Swift, Nonequilibrium melting and crystallization of a model Lennard-Jones system, *J. Chem. Phys.,* 120 (2004) 11640-11649.
[26] S. Nosé and F. Yonezawa, Isothermal-isobaric computer simulations of melting and crystallization of a Lennard-Jones system, *J. Chem. Phys.,* 84 (1986) 1803-1814.
[27] H. E. A. Huitema, M. J. Vlot and J. P. van der Eerden, Simulations of crystal growth from Lennard-Jones melt: Detailed measurements of the interface structure, *J. Chem. Phys.,* 111 (1999) 4714-4723.

Jae Dong Chung received his B.S. degree in Mechanical Engineering from Seoul National University, Korea, in 1990. He then received his M.S. and Ph.D. degrees from Seoul National University in 1992 and 1996, respectively. Dr. Chung is currently a Professor at the Mechanical Engineering at Sejong University in Seoul, Korea. He serves as a Director of General Affairs of the SAREK and the thermal division of KSME. Dr. Chung's research interests include nano-scale heat transfer, phase change, material processing and HVAC&R.